January, 1987] © *1987 The Chemical Society of Japan* *Bull. Chem. Soc. Jpn.*, ***60***, *9—18 (1987)*

Band Shape of Photoelectron Spectrum and Potential Energy Curve for Alkylamine

Masao Takahashi,* Iwao Watanabe, and Shigero Ikeda

Department of Chemistry, Faculty of Science, Osaka University,
Toyonaka, Osaka 560

(Received May 6, 1986)

Accurate measurements of UPS and ab initio potential energy calculations have been carried out for ammonia and several alkylamines to interpret the band shape of the UPS. Theoretical photoelectron band shape was obtained by a simple Franck-Condon approach. The calculation predicted very well the alkyl substitution effects on the ionization potentials and on the band widths of the first bands in UPS for the alkylamines. The following conclusions were obtained by comparing these theoretical photoelectron bands with experimental ones. The threshold ionization potential observed in the UPS is not always thermodynamically adiabatic ionization energy, but it can be subject to hot bands. Adiabatic ionization potential I_{Pa} of ammonia is concluded to be 10.08 eV. And the values of I_{Pa} for a series of alkylamines are evaluated by taking account of molecular vibrational frequency for the neutral state.

Though numerous investigations on UV photoelectron spectra (UPS) for free molecules have been executed, most of them have been concerned only with their ionization energies. We have been interested in the information obtainable from the band shape of the UPS. Our attention has been paid to the first band of the UPS corresponding to the ionization of a HOMO electron which must play the most important role with respect to the chemical reactivity of the molecule. The band shape of the UPS is related to the degree of distortion in the molecular structure after the photoionization, viz., the larger the distortion, the wider the band width.[1] The distortion also occurs after one-electron oxidation in solution, so that the degree of distortion must affect kinetics of electrochemical oxidation reaction. We obtained accurate UPS for a series of alkylamines,[2] and found that the band width of the first band for amine molecule correlates with one of the kinetic parameters, transfer coefficient (symmetry factor), for electrochemical oxidation reaction in solution and qualitatively showed that both the band width and the transfer coefficient reflect the character of potential energy curves for neutral and cationic state.[3]

Nitrogen skeleton of amine of the neutral state is known to be pyramidal[4,5] and that of the cationic state planar.[6,7] Thus the equilibrium structure of the amine cation radical differs substantially from that of the neutral one. It results in a broad first band in the UPS with a long vibrational progression though the HOMO, from which an electron is removed, is a nonbonding orbital consisting mainly of nitrogen 2p orbital. In order to discuss the band feature of the UPS, the Franck-Condon factor for the transition from the neutral to cationic potential energy surface is necessary. The Franck-Condon factors were calculated and reported for simple molecules[8,9] by many workers. The calculations for ammonia were also performed and the first band of its UPS was theoretically obtained.[10] However the potential energy surfaces of neutral alkylamines and the corresponding cation radicals are far more complex and have not yet been calculated.

One must also pay attention to whether the adiabatic ionization potential, I_{Pa}, can be determined from the UPS for the molecule which undergoes large change in its geometry after the photoionization process. For ammonia it remains uncertain whether the first peak in the vibrational progression for the first band corresponds to I_{Pa} or not.[6b,11] It is known that the photoionization processes corresponding to I_{Pa} are intrinsically unobservable for water dimer molecule[12] and van der Waals molecules composed of inert gas atoms.[9]

We carried out ab initio MO calculations for ammonia, mono-, di-, and trimethylamine and mono-, di-, and triethylamine, with several different geometries both for the neutral and cationic states and obtained potential energy curves on the deformation coordinate of the bending vibration. Theoretical photoelectron band can be derived from the potential energy curves by using a simple Franck-Condon approach. The band shape of UPS theoretically obtained will be compared with the experimental UPS data to test the validity of the present approach. The effects of the alkyl substitution on the band shape and ionization potentials are also studied.

Experimental

The experimental setup for the UPS measurements has been presented elsewhere[2] and will be outlined here. The ionization energy scale was calibrated with either argon (I_P=15.759 eV) or xenon (I_P=12.130 eV) used as an internal reference. The instrumental resolution was 20—30 meV. The spectrometer was kept at about 300 K and the temperature of the ionization chamber was higher by about 20 K because of the heat of a helium discharge lamp. For a low vapor pressure sample of tripentylamine the spectrometer was heated to 307 K to obtain sufficient vapor pressure. The spectral data for the first bands corresponding to the ionization of HOMO electron were accumulated more than 25 times. All the samples were commercial products and the samples obtained in the form of aqueous solutions were evaporated from the solution by adding sodium hydroxide.

Vertical ionization potential I_{Pv} was read at the maximum of the most intense vibrational component of the first band when vibrational progressions were well resolved. Threshold ionization potential I_{Pth} was read at the first vibrational peak of the band. For the molecule which displays no vibrational fine structure, I_{Pv} was read at the maximum of the band, and I_{Pth} was determined as follows. We took the point where the spectral intensity was 1% of the band maximum over the threshold region as the onset of the band. Then the I_{Pth} was obtained by adding 0.15 eV to the onset. 0.15 eV (0.148±0.017 eV) is the average distance between the onset and the first vibrational peak of the band for those molecules which display vibrational progressions. Bandwidth δ was determined from the full width at half-maximum (FWHM) of the first band. When the band displayed vibrational fine structure, the δ was read from the FWHM of the envelope connecting vibrational peaks. Though the accuracies of I_P and δ depend on the band shape, we believe that they are better than 0.02 eV.

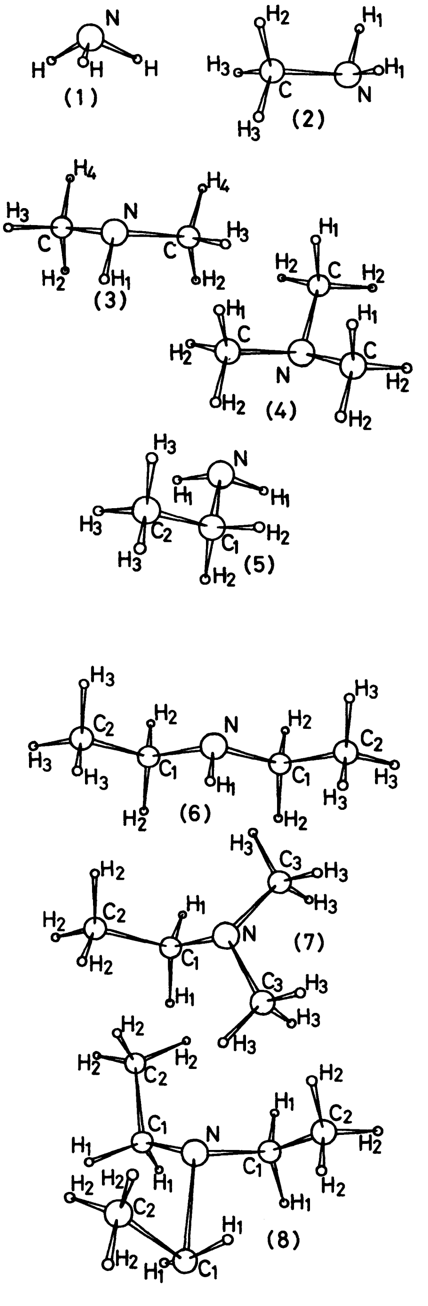

Fig. 1. Molecular geometries used for calculations for ammonia (1), methylamine (2), dimethylamine (3), trimethylamine (4), ethylamine (5), diethylamine (6), *N*,*N*-dimethylethylamine (7), and triethylamine (8).

Computational Procedure

In the present work, we performed ab initio MO calculations for ammonia, mono-, di-, and trimethylamine, *N*,*N*-dimethylethylamine and mono-, di-, and triethylamine. Calculations were carried out using the Gaussian 80 program and the IMSPACK program[13] with the minimal STO-3G basis set. For the cationic state, the open-shell calculations were performed with an unrestricted Hartree–Fock (UHF) procedure included in the programs.

The geometries for both neutral and cationic states were optimized by means of gradient method included in the Gaussian 80 program. The full-geometry optimizations were carried out except for diethylamine, *N*,*N*-dimethylethylamine and triethylamine, for which the structural parameters within ethyl group were fixed to the values optimized for ethylamine. The symmetries used for the calculations are; C_{3v} for ammonia and trimethylamine, C_3 for triethylamine, and C_s for all the others and also ammonia and trimethylamine. The optimized geometries are described in Fig. 1, and the structural parameters obtained are listed in Table 1. The bond lengths and angles are in good agreement with those obtained experimentally and calculated by others.[14]

As indicated in Table 1, the change in geometry of the cation radical from the neutral molecule is

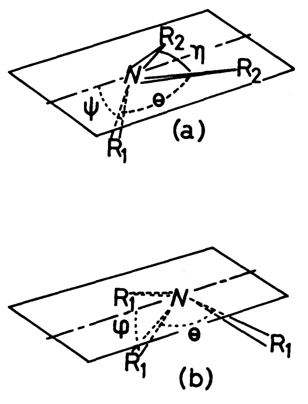

Fig. 2. Deformation angles and internal coordinates. R_1 and R_2 denote H, CH_3, or C_2H_5. (a) for C_s symmetry and (b) for C_3 and C_{3v}.

Table 1. Optimized Structural Parameters and Total Energy
(Bond length in nm, Bond angle in degree, and Energy in a.u.)

	Neutral state	Cationic state		Neutral state	Cationic state
Ammonia			Trimethylamine		
N-H	0.1033	0.1056	N-C	0.1485	0.1508
	(0.1006)			(0.1457)	
ϕ	24.4	0.0	C-H_1	0.1094	0.1094
	(0.0)			(0.1096)	
Total energy	−55.4554	−55.2070	C-H_2	0.1089	0.1091
	(−55.4377)			(0.1090)	
Methylamine			H_1-C-N	113.0	107.4
N-C	0.1486	0.1509		(113.1)	
	(0.1449)		H_2-C-N	109.3	108.6
N-H_1	0.1033	0.1054		(110.1)	
	(0.1009)		ϕ	18.6	2.7
C-H_2	0.1093	0.1098		(0.0)	
	(0.1096)		Total energy	−171.1919	−171.0214
C-H_3	0.1089	0.1093		(−171.1755)	
	(0.1091)		Ethylamine		
H_2-C-N	113.7	106.6	N-C_1	0.1490	0.1522
	(113.6)		C_1-C_2	0.1541	0.1544
H_3-C-N	109.1	107.9	N-H_1	0.1033	0.1053
	(110.2)		C_1-H_2	0.1093	0.1096
H_1-N-H_1 (η)	104.4	116.4	C_2-H_3	0.1086	0.1086
	(118.2)		C_2-C_1-N	110.5	109.1
ψ	60.9	0.0	H_2-C_1-N	110.1	105.6
	(0.0)		H_3-C_2-C_1	110.4	109.8
Total energy	−94.0329	−93.8167	H-N-H (η)	104.4	116.2
	(−94.0162)		ψ	61.5	0.0
Dimethylamine			Total energy	−132.6148	−132.4059
N-C	0.1485	0.1506	Diethylamine		
	(0.1452)		N-H_1	0.1033	0.1052
N-H_1	0.1034	0.1053	N-C_1	0.1488	0.1519
	(0.1011)		C_1-C_2	0.1542	0.1541
C-H_2	0.1091	0.1093	C_2-C_1-N	109.9	110.0
	(0.1095)		C_1-N-C_1 (η)	111.6	123.6
C-H_3	0.1089	0.1095	ψ	59.0	0.0
	(0.1089)		Total energy	−209.7757	−209.5970
C-H_4	0.1091	0.1093	*N*,*N*-Dimethylethylamine		
	(0.1095)		N-C_1	0.1498	0.1510
H_2-C-N	113.4	108.7	C_1-C_2	0.1547	0.1552
	(112.1)		N-C_3	0.1485	0.1500
H_3-C-N	109.0	107.4	C_2-C_1-N	110.6	108.0
	(109.4)		C_3-N-C_3 (η)	110.2	119.0
H_4-C-N	109.2	107.4	ψ	49.9	1.4
	(111.8)		Total energy	−209.7665	−209.6064
C-N-C (η)	111.2	125.8	Triethylamine		
	(121.2)		N-C_1	0.1494	0.1523
ψ	59.0	0.0	C_1-C_2	0.1545	0.1547
	(0.0)		C_2-C_1-N	111.1	111.6
Total energy	−132.6122	−132.4215	ϕ	18.4	2.1
	(−132.5968)		Total energy	−286.9283	−286.7754

ψ and ϕ are the angles defined in Fig. 2. Values in parenthesis are calculated for the planar form, i.e. ψ or $\phi=0°$. The following parameters are fixed for the neutral and the cationic state respectively, for diethylamine (H_2-C_1; 0.1093 and 0.1096, H_3-C_2; 0.1086 and 0.1087, H_2-C_1-N; 110.5 and 105.6, H_3-C_2-C_1; 110.5 and 110.0) and for triethylamine(C_1-H_1; 0.1093 and 0.1096, C_2-H_2; 0.1086 and 0.1087, H_1-C_1-N; 110.5 and 105.6, H_2-C_2-C_1; 110.5 and 110.0), and are fixed for both the neutral and the cationic states for *N*,*N*-dimethylethylamine (C_1-H_1; 0.1090, C_2-H_2; 0.1090, C_3-H_3; 0.1090, H_1-C_1-N; 110.0, H_2-C_2-C_1; 109.5, H_3-C_3-N; 110.0).

remarkable only in ψ or ϕ, which denotes the deformation angle as shown in Fig. 2. The first band of the UPS for the alkylamine has a very strong vibrational progression which corresponds to the deformation vibration. Thus we chose a potential energy curve on the coordinate of ψ or ϕ, for the calculation of theoretical band of the UPS. Potential energy curves were also calculated by using the angles HNH for methylamine and CNC for dimethylamine as the reaction coordinates. During the calculations other structural parameters were fixed at the optimized values for the neutral state.

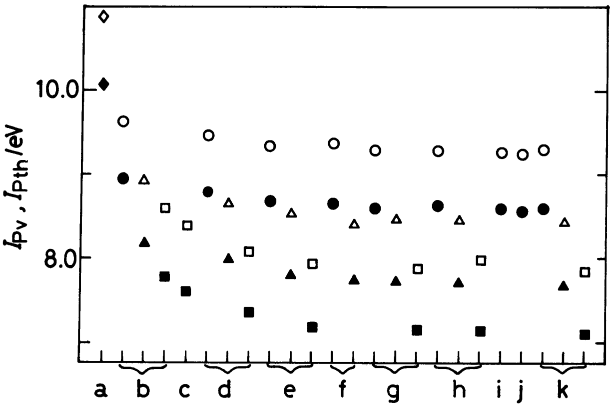

Fig. 3. Alkyl Substitution effect on I_{Pv} (open marks) and I_{Pth} (closed marks). Primary amines (○), secondary amines (△), tertiary amines (□), and ammonia (◇), (a) amomnia, (b) methyl-, (c) *N*,*N*-dimethylethylamine, (d) ethyl-, (e) propyl-, (f) isopropyl-, (g) butyl, (h) isobutyl-, (i) *s*-butyl,- (j) *t*-butyl-, and (k) pentyl-.

Results and Discussion

Observed Spectra. The He(I) photoelectron spectra of various alkylamines were previously reported.[2] The report includes their expanded first bands which are broad and are ascribable to the photoionization of a 2p non-bonding electron on nitrogen. Vibrational progressions are observed in the first bands for all the primary amines. The first bands for some of the secondary and tertiary amines also have vibrational structures. The vibrational frequencies listed in Table 2 are to be comparable to the ones for the neutral state and will be discussed in the following section. The vibrational structures are composed almost entirely of angle deformation mode and the other vibrational modes are only slightly observable, e.g., in the case of ammonia.[6b, 11]

The I_{Pv} and the I_{Pth} for alkylamines decrease in the order of primary, secondary and tertiary amine as shown in Fig. 3. They also decrease with the length of alkyl group from methyl to propyl and level off. The successive decrease in ionization potential up to

Table 2. Vibrational Frequencies(cm^{-1}) and Populations(%) on Each Vibrational Level (Populations are in Parenthesis)

State	Experiment	Calculation
	Ammonia	
Neutral	933$^{a)}$	1450
	($v''=0$; 99), ($v''=1$; 1)	($v''=0$; 99), ($v''=1$; 1)
Cationic	900	1690
	Methylamine	
Neutral	780$^{b,c,d)}$	1370$^{e)}$
	($v''=0$; 97), ($v''=1$; 3)	($v''=0$; 100)
	875$^{f)}$	
	($v''=0$; 98), ($v''=1$; 2)	
	1623$^{b,c,d)}$	2740$^{g)}$
	($v''=0$; 100)	($v''=0$; 100)
Cationic	880	1330
	Dimethylamine	
Neutral	383$^{b,d)}$	670$^{g)}$
	($v''=0$; 84), ($v''=1$; 14), ($v''=2$; 2)	($v''=0$; 95), ($v''=1$; 5)
	735$^{b,d)}$	1130$^{e)}$
	($v''=0$; 96), ($v''=1$; 4)	($v''=0$; 99), ($v''=1$; 1)
Cationic	~520	1050
	Trimethylamine	
Neutral	366$^{b,d,h)}$	580
	($v''=0$; 88), ($v''=1$; 16), ($v''=2$; 2)	($v''=0$; 92), ($v''=1$; 7), ($v''=2$; 1)
Cationic	~400	660

Experimental values for the cationic state are collected in this work, see also Ref. 2. a) Refs. 4 and 15a. b) Ref. 33. c) Ref. 34. d) Ref. 35. e) Vibrational mode corresponding to ψ. f) Observed in Raman spectrum, taken from Ref. 36. g) Vibrational mode corresponding to η. h) Ref. 19.

propyl substitution indicates that for the amine with smaller alkyl groups, the cationic state is stabilized to a greater extent than the neutral state by the introduction of a longer alkyl group. It is a case for a series of aliphatic alcohols, in which the I_P values continue to decrease up to butyl substitution.[29] It seems that oxygen atom being more electronegative than nitrogen exhibits electron-attracting effect extending to longer range in alcohol than that in amine.

The half width δ of the first band decreases in the order of primary, secondary, and tertiary amine as shown in Fig. 4. The systematic decrease of δ with the length of alkyl group is also indicated. However there is unexpected behavior of I_P shown in the same figure that the value of $\Delta I_{Pv,th}$, the difference between I_{Pv} and I_{Pth}, does not exhibit such trend against the alkyl substitution. We will discuss the behavior of $\Delta I_{Pv,th}$ in the following section.

Potential Energy Curves. The potential energy curves calculated for the neutral and cationic state are shown in Figs. 5 and 6. The potential energy V used in this paper is referred to the minimum of the total energy for the neutral state. Potential energy curves shown in Fig. 5 are obtained by varying ψ under C_s symmetry and those in Fig. 6a by varying ϕ under symmetry of C_{3v} for ammonia and trimethylamine and C_3 for triethylamine.

Though the potential energy curves for neutral methylamine (2) and ethylamine (5) almost overlap as shown in Fig. 5, the curve for ethylamine cation radical is steeper than that for methylamine cation radical, and this is due to the fixed geometry within the ethyl group. Same trend is seen in the case of dimethylamine (3) or diethylamine (6).

As can be seen in Fig. 5, trimethylamine (4) and *N,N*-dimethylethylamine (7) have steeper curves at the larger $|\psi|$ for both the neutral and the cationic state. This is considered to be due to the steric hindrance of the bulky substituent group.

The geometries optimized for neutral ammonia and the methyl amines with planar nitrogen skeleton are included in Table 1. Obvious difference in CN and/or HN bond lengths exists between the molecules with the pyramidal and the planar nitrogen skeletons. These bonds are longer in the pyramidal form than in the planar form. The differences in total energy between the pyramidal and the planar form for the neutral state are 0.48, 0.45, 0.42, and 0.45 eV for ammonia, methylamine, dimethylamine, and trimeth-

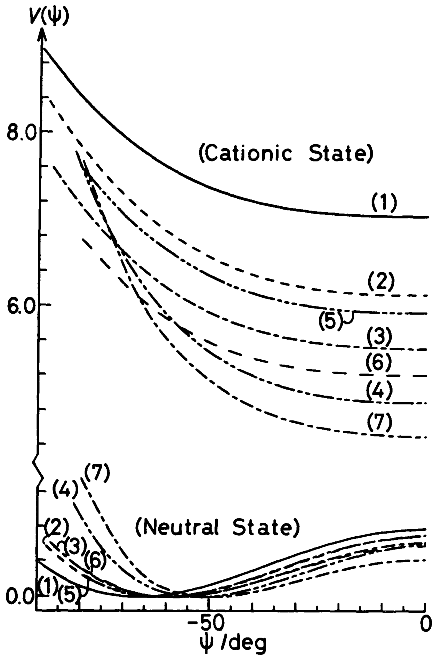

Fig. 5. Potential energy curves for ammonia and several alkylamines, against ψ under C_s symmetry. The notations 1 to 8 are the same as in Table 3. The molecular symmetry of (5) is C_1.

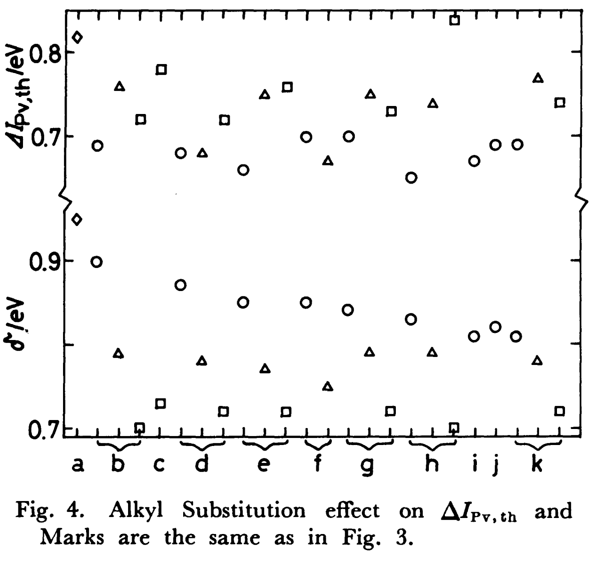

Fig. 4. Alkyl Substitution effect on $\Delta I_{Pv,th}$ and δ. Marks are the same as in Fig. 3.

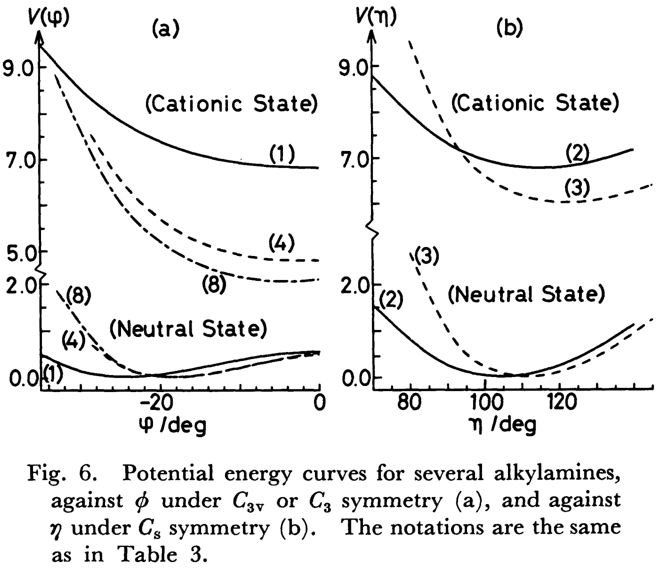

Fig. 6. Potential energy curves for several alkylamines, against ϕ under C_{3v} or C_3 symmetry (a), and against η under C_s symmetry (b). The notations are the same as in Table 3.

ylamine, respectivery. The differences corresponding to the amino inversion barrier are larger than those previously reported.[5a, 30] The barriers determined from Figs. 5 and 6a are even higher because the geometries at ψ or $\phi=0°$ are not energetically optimized.[31] Furthermore neglect of configuration interaction (CI) and lack of superior basis sets may well make the potential energy curves calculated here different from the actual ones. However, the fact that the MO calculations predict the drastic change on ψ or ϕ coordinate after the ionization suggests that the most important part of the intrinsic characters of the vibration induced by photoionization are describable with the present potential energy curves.

Potential energies as a function of the angle η were also calculated for methylamine and dimethylamine and are given in Fig. 6b. Although the value of η for each cation radical with the most stable geometry in the figure is different by about 10 degrees from that for the optimized geometry of neutral molecule, the curves for cation radical and neutral molecule are similar indicating that the deformation in η after the photoionization is small.

Band Shape of the Theoretical Photoelectron Spectrum. In order to obtain an envelope of a theoretical photoelectron band, we have carried out a following simple approach. First of all, we connected ψ or ϕ with an internal coordinate θ. A harmonic oscillator approximation on $V(\theta)$ gives a force constant and then a vibrational frequency is calculated by use of Willson's ***GF*** matrix method.[32] A wave function Ψ for the harmonic vibration is also calculated. Although it is well-known that an unharmonicity exists in the deformational vibration of amine at the large amplitude, we have neglected the unharmonic terms because of the simplicity of the calculation. Next, assuming a Boltzmann distribution at 320 K which is the temperature of the ionization chamber, the population p_i on each vibrational state i is obtained. The calculated frequencies and the populations are collected in Table 2 together with the experimental frequencies for ammonia and mono-, di-, and trimethylamine. Values of calculated frequencies are not in agreement with experimental ones. However, the following facts indicate that the essential property of molecular vibration in alkylamines concerned remains in the present potential energy curves; both experiment and calculation are in agreement on the point that the NH_2 wagging frequency is lower than the symmetric NH_2 deformational frequency for methylamine and that the CNC skeletal deformational frequency is lower than the a′ N–H deformational frequency for dimethylamine.

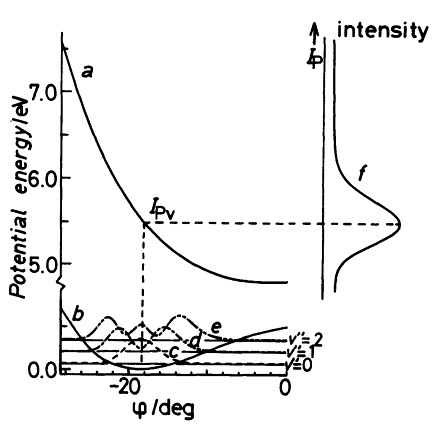

Fig. 7. Potential energy curves for the neutral (*b*) and the cationic (*a*) state of trimethylamine, the square of the wave function (Ψ_1^2) (*c*, *d* and *e*), and the photoelectron band (*f*) evaluated from them.

Now the theoretical photoelectron band *f* shown in Fig. 7 is obtained as follows. The curve *c*, Ψ_0^2, is projected on the potential energy curve *a* for cation radical and weighted with p_0 for the $v''=0$ state. This gives us the photoelectron spectrum intensity corresponding to the ionization from $v''=0$. Then the photoelectron spectrum *f* is obtained as the accumulation of all the ionizations from the vibrational states whose population is larger than 1%. In Fig. 8 are shown the theoretical photoelectron spectra for amines calculated in this work. In the figure, each spectrum is shifted in energy so that the maximum corresponding to I_{Pv} comes on the same position on abscissa. It is assumed for the simplicity of the

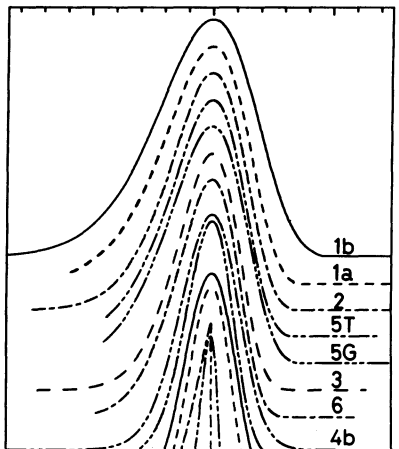

Fig. 8. Theoretical photoelectron band. The numerical notations are the same as in Table 3.
a; calculated under C_s symmetry and b; calculated under C_{3v} symmetry. T; trans conformation, G; gauche conformation. c; the curves noted with c are band shapes calculated under the assumption that only the coordinate of η vibrates.

theoretical treatment that the vibrational levels for the cationic state are continuous. This is not correct from the quantum chemical point of view. However because the vibrational symmetries for the neutral and cationic molecules are same, the curve obtained in this manner should be comparable to the envelope of the experimental photoelectron spectrum. In Fig. 8 are also shown the theoretical photoelectron bands arising from the vibration on η for methylamine and dimethylamine. Both of them are sharp and I_{Pth} is equal or close to I_{Pv}. This indicates that this kind of vibration less contributes to the band shape.

The band width δ and threshold energy I_{Pth} are determined from the theoretical photoelectron bands. The I_{Pth} is read at the onset whose intensity is 1% of the band maximum. Table 3 contains the theoretical values for δ, I_{Pth}, I_{Pa}, and I_{Pv}, together with experimental ones. The I_{Pv}(ΔSCF) is defined as a difference in total energy between the neutral and the cationic state with the same geometry which is the most stable for the neutral state. The I_{Pa} is defined as a difference in minimum total energy between the neutral and the cationic state each with the most stable geometry.

The calculated values of I_{Pth} are always larger than those of calculated I_{Pa}. This owes to the fact that the I_{Pa} is the difference in total energy between optimized geometries for the neutral and cationic state, while the I_{Pth} is evaluated by use of the potential energy curves as a function of only ψ or ϕ. That makes the total energy for cation radical at the minimum-energy point on the potential energy curve more unstable than that with the optimized geometry.[31] The theoretical values of I_{Pv}, I_{Pa}, and I_{Pth} are underestimated, and if a constant value of 3.1 eV is added to the theoretical values of I_{Pv}, they are in excellent agreement with the experimental ones. The calculations also predict the values of δ very well as shown in Fig. 9 in which the theoretical and experimental values are compared.

Band Width. The band width and the band shape depend on the following factors: (i) The difference in geometry between the neutral and cationic molecule each with the most stable geometry; (ii) the vibrational wave function for the neutral state which is based on the feature of the potential energy curve for the neutral state; (iii) the slope of the potential energy curve for the cationic state.

The calculated δ must be underestimated because the potential energy at minimum on the potential energy curve for cation radical is higher than that for the cation radical with the optimized geometry,[31] i.e., the potential energy curve for cation radical should be steeper. For ammonia and trimethylamine we have obtained the theoretical photoelectron band by two methods. One is the use of the potential energy curve for C_{3v} symmetry and the other is the use of C_s symmetry, i.e., the potential energy curve obtained as a function of ψ, while fixing the angle η to the value for the optimized geometry for the neutral state (1b and 4b in Fig. 8). δ's evaluated under the C_s symmetry have reproduced the experimental values more poorly

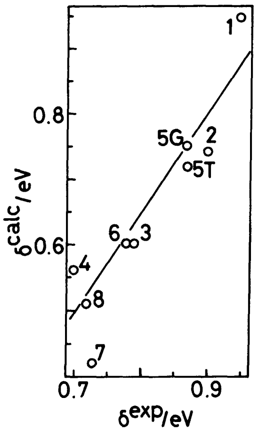

Fig. 9. Comparison between experimental and calculated δ. The notations are the same as in Table 3. G; gauche conformation. T; trans conformation.

Table 3. Experimental and Theoretical Ionization Potentials and Bandwidths (δ) (in eV)

	I_{Pv}		I_{Pa}[a]	I_{Pth}		δ		$\Delta I_{Pv,a}$	$\Delta I_{Pv,a}$[b]	I_{Pa}[c]	I_{Pa}[d]
	exp	calcd	calcd	exp	calcd	exp	calcd	calcd	corr	corr	corr
1) Ammonia	10.90	7.79	6.76	10.08	6.91	0.95	0.95	1.03	—	—	—
2) Methylamine	9.64	6.86	5.88	8.95	6.19	0.90	0.74	0.98	0.68	8.96	8.95
3) Dimethylamine	8.94	6.15	5.19	8.18	5.55	0.79	0.60	0.96	0.66	8.28	8.27
4) Trimethylamine	8.51	5.54	4.64	7.79	4.84	0.70	0.56	0.90	0.60	7.91	7.89
5) Ethylamine	9.46	6.67	5.68	8.78	5.98	0.87	0.75	0.99	0.69	8.77	8.78
6) Diethylamine	8.67	5.80	4.86	7.99	5.25	0.78	0.60	0.94	0.64	8.03	8.08
7) *N*,*N*-Dimethylethylamine	8.39	5.11	4.36	7.61	4.61	0.73	0.42	0.75	0.45	7.49	7.71
8) Triethylamine	8.09	5.02	4.16	7.37	4.42	0.72	0.51	0.86	0.56	7.53	7.47

a) The difference in total energies of the neutral molecule and the cation radical each with equilibrium geometry. b) Corrected $\Delta I_{Pv,a}$. c) $I_{Pv}^{exp}-\Delta I_{Pv,a}^{corr}$. d) Determined by adding the energy of a vibrational quanta to I_{Pth}^{exp}, see text.

than those under the C_{3v} symmetry. This is chiefly due to the fixed angle η.

As shown in Fig. 9 the deviation from the correlation line between experimental and calculated values is large for the case of *N,N*-dimethylethylamine. δ for this amine is quite underestimated because of the fixed CNC skeleton the same as the case of trimethylamine calculated under C_s symmetry. There is some limitation in the present method to estimate band width of the UPS, because the potential energy curve used is a cross section of potential energy hypersurface taken only on a single coordinate on which the change after the photoionization is greatest.

Threshold Ionization Potential and Potential Energy Curve. The I_{Pth} mainly depends on the next three factors: (I) The difference in the geometry between the neutral molecule and the cation radical each with the most stable structure; (II) the population on each vibrational level for the neutral state; (III) the value of vibrational probability density Ψ_0^2 for the neutral state with the geometry similar to the equilibrium geometry for the cationic state. When the difference for (I) is large, I_{Pa} may well be smaller than I_{Pth} and intrinsically undetectable in UPS. While the larger population on a higher vibrational level causes larger probability of hot band. When the value for (III) is large, I_{Pa} should be detectable. Note that even if the value for (I) is large, the large value for (III) makes I_{Pa} detectable.

It is interesting that although it is impossible to predict the values of $\Delta I_{Pv,th}$ accurately from the theoretical potential energy curves, the values of δ are predicted excellently from the curves as shown in Fig. 9 (except *N,N*-dimethylethylamine). This implies that the present potential energy curve for cation radical is distorted only around the equilibrium geometry for cation radical. With respect to *N,N*-dimethylethylamine, both δ and $\Delta I_{Pv,th}$ deviate from the correlation between experimental and calculated values. Thus the slope on the calculated curve for *N,N*-dimethylethylamine cation radical is gentler than the actual curve.

While I_P and δ systematically vary in the order of primary, secondary and tertiary amine, $\Delta I_{Pv,th}$ does not. This can be interpreted as follows. The populations on the higher vibrational levels for the neutral state increase in the order of primary, secondary and tertiary amine, since the vibrational frequency decreases in the same order. On the other hand the probability density Ψ_0^2 at the most stable geometry of cation radical decreases in the order of primary, secondary and tertiary amine. The two opposing factors result in the unsystematic order of $\Delta I_{Pv,th}$ as shown in Fig. 4.

Determination of Adiabatic Ionization Potential. The first ionization peak 10.075 eV in the UPS of ammonia, observed also by several other workers,[6b,7,11] has been regarded as the hot band.[6b,7] Population on $v''=1$ is, however, 1% as listed in Table 2, and the ratio of Ψ_1^2 to Ψ_0^2 at the equibrium geometry of ammonia cation radical is very small. Thus $0\leftarrow1$ ionization peak, i.e., hot band, should be indiscernible in the UPS. If the first peak were the $0\leftarrow1$ ionization peak, intensity of the first peak should be a few hundredth of that of the second peak according to Boltzmann distribution, since ionization cross section for the same vibrational mode is similar. The ratio of the first peak height to the second in the UPS is 0.24 and is too large to assign the first peak to $0\leftarrow1$ ionization peak. Then we conclude that the first peak is not the $0\leftarrow1$ but the $0\leftarrow0$ ionization peak, and that I_{Pa} is 10.08 eV. As for primary amines, the frequency of deformation vibration of ψ, viz., NH_2 wagging vibration, is in the range of 850—750 cm^{-1} from the infrared spectra of liquid phase,[36] so the population on $v''=1$ should be 2—4%. Peak height of the first peak in the vibrational progression in the first band for methylamine and ethylamine, compared to that of the second peak, however, is too large to assign the first peak to $0\leftarrow1$ ionization peak. Therefore the first peaks for methylamine and ethylamine pertain to the $0\leftarrow0$ ionization peak and the I_{Pa}'s are 8.95 and 8.78 eV, respectively.

Now we estimate I_{Pa}'s for mono-, di-, and trimethylamine and the ethylamines by use of I_{Pa}^{calcd} calculated here and experimental I_{Pth}^{exp}. I_{Pa}^{calcd} is largely underestimated because of the neglect of CI and the lack of superior basis set. So is I_{Pv}^{calcd}, but one expects that this is somewhat canceled out in the difference $\Delta I_{Pv,a}^{calcd}(=I_{Pv}^{calcd}-I_{Pa}^{calcd})$. $\Delta I_{Pv,a}^{corr}$ is obtained by adding 0.30 eV to $\Delta I_{Pv,a}^{calcd}$. The correction of 0.30 eV gives $\Delta I_{Pv,a}^{calcd}$ equal to $\Delta I_{Pv,th}^{exp}$ for methylamine and ethylamine. Finally I_{Pa} is estimated by subtracting $\Delta I_{Pv,a}^{corr}$ from I_{Pv}^{exp}. The values of I_{Pa} are included in Table 3 together with $\Delta I_{Pv,a}^{calcd}$ and $\Delta I_{Pv,a}^{corr}$. The difference between I_{Pa} and I_{Pth}^{exp} are 0.12 and 0.16 eV for trimethylamine and triethylamine, respectively. These values indicate that the hot band should be observable and that the hot band can be at least $0\leftarrow2$ ionization peak if considered that the frequency of the vibration of ϕ for neutral trimethylamine and triethylamine is about 0.05 eV.[36] For diethylamine the difference between I_{Pa} and I_{Pth}^{exp} is 0.05 eV, and this indicates that the hot band may be observable, or that the difference is only the error produced in the calculation because the frequency of the vibration of ψ is about 0.09 eV.[36] The difference for dimethylamine is 0.09 eV, and the hot band, $0\leftarrow1$ ionization peak, may exist. However, the hot band should not be observabvle, if the population p_1 and probability density Ψ_1^2 of the neutral state at the equilibrium geometry of the cation radical are considered. The hot band of dimethylamine may be due to the coupling of the vibration of ψ with other

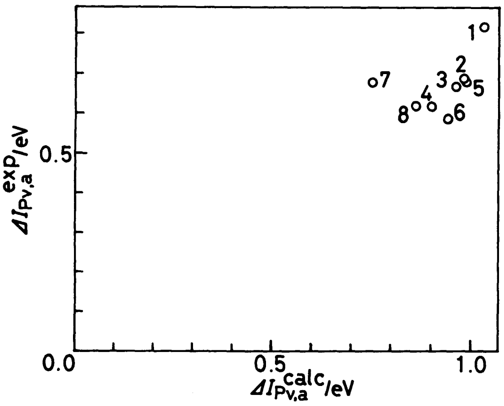

Fig. 10. Comparison between experimental and calculated $\Delta I_{Pv,a}$. The notations are the same as in Table 3.

vibrations.

According to the discussions one can estimate the thermodynamic I_{Pa} by combining photoelectron spectroscopic I_{Pth} and vibrational energy. Assuming that 0←1 and 0←2 ionizations are observable for the secondary and the tertiary amines, respectively, the values for I_{Pa} are obtained by adding 0.09 eV to I_{Pth} for the secondary and 0.10 eV for the tertiary amines and are listed in Table 3. By using the I_{Pa} obtained in this manner, we can obtain the values of $\Delta I_{Pv,a}{}^{exp}$, which are compared with the theoretical $\Delta I_{Pv,a}$'s in Fig. 10. The correlation indicates that 0.3 eV subtraction from the theoretical value predicts the experimental one excellently, except for ammonia, triethylamine and *N*,*N*-dimethylethylamine. This result also supports the present determination of the thermodynamic I_{Pa} for amines.

The authors wish to thank Professor Takayuki Fueno and Dr. Kizashi Yamaguchi, Department of Chemistry, Faculty of Engineering Science, Osaka University for the computer program of the IMSPACK revised for the computer in Osaka University. The calculations were carried out using HITAC M-200H at the computer center of IMS (Institute for Molecular Science) and ACOS NEAC 1000 at the computation center, Osaka University.

References

1) J. H. D. Eland, "Photoelectron Spectroscopy," Butterworth and Co., London (1974), Chap. 5.

2) M. Takahashi, I. Watanabe, and S. Ikeda, *J. Electron Spectrosc. Relat. Phenom.*, **37**, 275 (1985).

3) M. Takahashi, I. Watanabe, and S. Ikeda, *J. Phys. Chem.*, **87**, 5059 (1983).

4) G. Hertzberg, "Infrared and Raman Spectra of Polyatomic Molecules II. Infrared and Raman Spectra of Polyatomic Molecules," D. Van Nostrand Co., New York (1945).

5) a) R. A. Eades, D. A. Weil, D. A. Dixon, and C. H. Douglass, Jr., *J. Phys. Chem*, **85**, 976 (1981); b) S. Profeta, Jr. and N. L. Allinger, *J. Am. Chem. Soc.*, **107**, 1907 (1985).

6) a) A. D. Walsh and P. A Warsop, *Trans. Faraday Soc.*, **57**, 345 (1961); b) A. W. Potts and W. C. Price, *Proc. R. Soc. London, Ser. A*, **326**, 181 (1972).

7) D. H. Aue, H. M. Webb, and M. T. Bowers, *J. Am. Chem. Soc.*, **97**, 4136 (1975).

8) M. E. Wocks, *J. Chem. Phys.*, **41**, 930 (1964); b) T. E. Sharp and H. M. Rosenstock, *J. Chem. Phys.*, **41**, 3453 (1964); c) M. Halmann and I. Laulicht, *J. Chem. Phys.*, **43**, 1503 (1965).

9) a) P. M. Dehmer and J. L. Dehmer, *J. Chem. Phys.*, **69**, 125 (1978); b) P. M. Dehmer and J. L. Dehmer, *J. Chem. Phys.*, **68**, 3462 (1978).

10) a) W. R. Harshbarger, *J. Chem. Phys.*, **53**, 903 (1970); b) *ibid*, **56**, 177 (1972); c) P. Avouris, A. R. Rossi, and C. Albrecht, *J. Chem. Phys.*, **74**, 5516 (1981).

11) J. W. Rabalais, L. Karlsson, L. O. Werme, T Bergmerk, and K. Siegbahn, *J. Chem. Phys.*, **58**, 3370 (1973).

12) a) S Tomoda and K. Kimura, *Chem Phys.*, **82**, 215 (1983); b) S. Tomoda and K. Kimura, *Chem. Phys. Lett.*, **111**, 434 (1984); c) S. Tomoda and K. Kimura, *Chem. Phys. Lett.*, **121**, 159 (1985).

13) K. Morokuma, S. Kato, K. Kitaura, I. Ohmine, S. Sakai, and S. Obara, IMS Computer Center Library, Institute for Molecular Science, No. 0372 (1980).

14) The calculated bond lengths and angles for ammonia, and mono-, di-, and trimethylamine agree with the experimental values[4,15–19] within a few hundredths of an angstrom and within a few degrees. The structural parameters for ethylamine are similar to those used in Ref. 20b. For mono-, di-, and triethylamine, the calculated conformations of the neutral state are in agreement with the result of experiment as follows. Most stable conformation of ethylamine has been reported to be either G (gauche) conformation with respect to the lone pair of the nitrogen,[20] or T (trans) conformation.[21] We have found that the G conformation is the most stable. However, the energy difference between these two conformations is only 8 meV which is less than the noise level of the computational technique, which is also stated in Ref. 5b. Diethylamine takes TT (trans–trans) conformation, i.e., each ethyl group has a methyl group at trans position with respect to the other ethyl group.[22] Triethylamine takes G′G′G′ conformation, i.e., each of the methyl group comes to the gauche position against the lone pair and other ethyl groups.[23] While another stable conformations were reported to be present,[23,24] we have taken the conformation of this molecule as G′G′G′ which is the result of the present geometry optimization. The structural parameters for the neutral ammonia and mono-, di-, and trimethylamine are in good agreement with those calculated by others.[5,25–27] The conformations calculated by L. Radom et al.[28] for the neutral methylamine, dimethylamine and ethylamine are in reasonable agreement with the present results. For ethylamine cation radical the difference in total energy between T conformation and G conformation has been only 3 meV.

15) a) W. S. Benedict and E. K. Plyler, *Can. J. Phys.*, **35**, 1235 (1957); b) Y. Morino, K. Kuchitsu, and S. Yamamoto, *Spectrochim. Acta*, **24A**, 235 (1968); c) K. Kuchitsu, J. P.

Guillory, and L. S. Bartell, *J. Chem. Phys.*, **49**, 2488 (1968).

16) a) T. Nishikawa, T. Itoh, and K. Shimoda, *J. Chem. Phys.*, **23**, 1735 (1955); b) D. R. Lide, Jr., *J. Chem. Phys.*, **27**, 343 (1957); c) H. K. Higginbotham and L. S. Bartell, *J. Chem. Phys.*, **42**, 1131 (1964); d) K. Takagi and T. Kojima, *J. Phys. Soc. Jpn.*, **30**, 1145 (1971).

17) a) J. E. Wollrab and V. W. Laurie, *J. Chem. Phys.*, **48**, 5058 (1968); b) B. Beagley and T. G. Hewitt, *Trans. Faraday Soc.*, **65**, 2565 (1968).

18) a) D. R. Lide, Jr. and D. E. Mann, *J. Chem. Phys.*, **28**, 572 (1958); b) J. E. Wollrab and V. W. Laurie, *J. Chem. Phys.*, **51**, 1580 (1969).

19) J. N. Gayles, *Spectrochim. Acta.*, **23A**, 1521 (1967).

20) a) P. J. Krueger and J. Jan, *Can. J. Chem.*, **48**, 3229 (1970); b) A. S. Manocha, E. C. Tuazon, and W. G. Fateley, *J. Phys. Chem.*, **78**, 803 (1974).

21) a) J. R. Durig and Y. S. Li, *J. Chem. Phys.*, **63**, 4110 (1975); b) M. Tsuboi, K. Tamagake, A. Y. Hirakawa, J. Yamaguchi, H. Nakagawa, A. S. Manocha, E. C. Tuzan, and W. G. Fateley, *J. Chem. Phys.*, **63**, 5177 (1975).

22) A. L. Verma, *Spectrochim. Acta, Part A*, **27A**, 2433 (1971).

23) C. H. Bushweller, S. H. Fleischman, G. L. Grady, P. McGoff, C. D. Rithner, M. R. Whalon, J. G. Brennan, R. P. Marcantonio, and R. P. Domingye, *J. Am. Chem. Soc.*, **104**, 6224 (1982).

24) K. Kamur, *Chem. Phys. Lett.*, **9**, 504 (1971).

25) a) A. Rauk, L. C. Allen, and E. Clementi, *J. Chem. Phys.*, **52**, 4133 (1970); b) W. A. Lathan, W. J. Hehre, L. A. Curtiss, and J. A. Pople, *J. Am. Chem. Soc.*, **93**, 6377 (1971); c) D, J. Defrees, B. A. Levi, S. K. Pollack, W. J. Hehre, J. S. Binkley and J. A. Pople, *J. Am. Chem. Soc.*, **101**, 4085 (1979); d) W. R. Rodwell and L. Radom, *J. Chem. Phys.*, **72**, 2205 (1980); e) P. Puley, G. Forarasi, F. Pang, and J. E. Boggs, *J. Am. Chem. Soc.*, **101**, 2550 (1979).

26) a) P. Pulay and E. Török, *J. Mol. Struct.*, **29**, 239 (1975); b) E. Flood, P. Puley, and J. E. Boggs, *J. Am. Chem. Soc.*, **99**, 5570 (1977).

27) S. Skaarup, L. L. Griffin, and J. E. Boggs, *J. Am. Chem. Soc.*, **98**, 3140 (1976).

28) L. Radom, W. J. Hehre, and J. A. Pople, *J. Am. Chem. Soc.*, **94**, 2371 (1972).

29) A. D. Baker, D. Betteridge, N. R. Kemp, and R. E. Kirby, *Anal. Chem.*, **43**, 375 (1971).

30) J. M. Lehn, *Fortchr. Chem. Forsch.*, **15**, 311 (1970).

31) Because of the fixed structural parameters except ψ or ϕ, minimum total energies of the cation radicals on the present potential energy curves are higher than those with the optimized geometries by the following values; 0.04 eV for ammonia, 0.23 eV for methylamine, 0.29 eV for dimethylamine, 0.14 eV for trimethylamine, 0.22 eV for ethylamine both with G and T conformations, 0.32 eV for diethylamine, 0.12 eV for *N*,*N*-dimethylethylamine, and 0.18 eV for triethylamine.

32) E. B. Wilson, Jr., J. C. Decius, and P. C. Cross, "Molecular Vibrations," McGraw-Hill Inc., New York (1980).

33) G. Dellepine and G. Zerbi, *J. Chem. Phys.*, **48**, 3573 (1968).

34) A. Y. Hirakawa, M. Tsuboi, and T. Shimanouchi, *J. Chem. Phys.*, **57**, 1236 (1972).

35) From infrared spectra for mono-, di-, and trimethylamine, of Refs. 33 and 34, the bond angle deformation frequencies about nitrogen skeleton are as follows: for methylamine, 780 cm^{-1} corresponding to mainly θ and partly to η, and 1623 cm^{-1} corresponding to mainly η and partly to θ; for dimethylamine 383 cm^{-1} corresponding to mainly η and partly to θ and to torsional angle around C–N axis, and 735 cm^{-1} corresponding to mainly θ and partly to C–N bond length; for trimethylamine 366 cm^{-1} dominantly corresponding to θ. In Raman spectra similar vibrations have also been reported.[36]

36) F. R. Dollish, W. G. Fateley, and F. F. Bentley, "Characteristic Raman Frequencies of Organic Compounds," Wiley-Interscience, N. Y. (1973).